AN INVESTIGATION OF STANDING WAVES USING A FULLY NON-LINEAR BOUNDARY ADAPTIVE FINITE ELEMENT METHOD

D M Greaves[1], A G L Borthwick[2] and G X Wu[1]

[1] Dept of Mechanical Engineering, University College London, Torrington Place, London WC1E 7JE, U.K.
[2] Dept of Engineering Science, University of Oxford, Parks Road, Oxford OX1 3PJ, U.K.

1. INTRODUCTION

This paper describes a quadtree based finite element solver for two-dimensional fully non-linear time-dependent free surface flows. In the scheme, the free surface is allowed to deform, and a new mesh created at each time step. To ensure fast, fully automatic mesh generation, an underlying Cartesian quadtree grid is first created about seeding points at the free surface and on rigid boundaries; the quadtree grid is then triangularised to generate the finite element mesh.

Details of the governing equations and finite element formulation used in this work are given by Wu and Eatock Taylor (1994, 1995). The quadtree-based grid generation is described in detail by Greaves (1995). Numerical results obtained here are for standing waves in rectangular tanks of various aspect ratio. The results show encouraging agreement with analytical solutions and alternative numerical data.

2. RESULTS

The fully non-linear moving boundary finite element method was used to simulate various cases of standing waves in rectangular containers. Mesh size and time step convergence tests were carried out for a steep standing wave profile, taken from Mercer and Roberts (1992). Standing waves generated from sinusoidal initial profiles were also considered. The decrease in non-linear wave frequency with amplitude in deep water, and the corresponding increase in shallow water, noted by Tsai and Jeng (1994) as well as Vanden-Broeck and Schwartz (1981) and Tadjbakhsh and Keller (1960), are observed. Each of the standing wave simulations presented herein has a larger crest amplitude than trough amplitude, which is typical of non-linear wave profiles (Tsai and Jeng, 1994).

The various parameters used in the numerical simulations are non-dimensionalised as follows,

$$\phi = \frac{\phi^*}{h^*\left(g^* h^*\right)^{\frac{1}{2}}}, \quad L = \frac{L^*}{h^*}, \quad t = \left(\frac{g^*}{h^*}\right)^{\frac{1}{2}} t^*, \quad \omega = \left(\frac{h^*}{g^*}\right)^{\frac{1}{2}} \omega^* \quad , \qquad (17)$$

where ϕ is the velocity potential, h is the water depth, g is the acceleration due to gravity, L is any length, t is time and ω is the wave frequency. The superscript * represents a dimensional value. All calculations were performed on a SUN SPARC 10 workstation.

In each of the following simulations, the dimensionless height of the container walls is equal to 1.5. Unless otherwise stated, the seeding points are spaced to provide the maximum mesh resolution along the free surface boundary and at the container walls in the region which intersects with the free surface. The seeding point spacing at the free surface is equal to $S_{min}=2^{-M}$, where M is the maximum division level of the underlying quadtree grid. Thus, the resolution of the underlying quadtree grid, and also of the finite element mesh, is finest where velocity potential gradients are likely to be highest, and coarsest at the bottom of the container where gradients are likely to be low.

Standing Waves in a Rectangular Container

Various standing waves were simulated in order to investigate the relationship between water depth, amplitude, and frequency of oscillation. The waves have initial surface elevation profile, $\eta = a\cos(2\pi x/b)$ where x is measured along the length of the tank, b is the length of the tank and a is the wave amplitude.

Figure 1 shows the initial mesh for case A. The dimensionless length of the tank, b, is equal to the dimensionless wavelength 2. The dimensionless wave amplitude, $a = 0.05$. Figure 2 shows the wave surface elevation history at the centre of the tank, plotted with the linear and first plus second order analytical solutions calculated following the method described by Wu and Eatock Taylor (1995), for comparison. The linearised analytical solution does not agree well with the fully non-linear numerical solution as time increases. The inclusion of second order terms, however, leads to much better agreement.

The time period of non-linear oscillation in Figure 2 is greater than that predicted by linear theory. This effect was noted by Tsai and Jeng (1994), Vanden-Broeck and Schwartz (1981), and Tadjbakhsh and Keller (1960). Tsai and Jeng (1994) calculated numerical Fourier solutions of standing waves in finite water depth, and observed that the non-linear wave frequency increases with wave steepness for water depths less than 0.1662 of its wavelength, and decreases with increasing amplitude for depths greater than this value.

Various cases were investigated and the results recorded in Table 1. Figure 3 shows the initial mesh for case D, and the temporal free surface elevation plot is given in Figure 4. In Figure 4, the third trough is higher than those surrounding it, which may indicate the occurrence of double minima in the wave profile at this stage. This effect is recorded by Tsai and Jeng (1994) for shallow water standing waves.

Each simulation was continued over at least five cycles and the non-linear wave frequency, ω, determined, along with the corresponding h/L_o and H/L_o values, where H is the wave height. The corresponding linear wave frequency, ω_o, and linear wave length, L_o, are calculated using linear wave theory. The ratio, ω/ω_o, is given in Table 1 as a function of h/L_o and H/L_o for each of the standing wave calculations and can be seen to agree reasonably with equivalent frequency ratios obtained from Tsai and Jeng's (1994) data. The decrease in non-linear wave frequency with increasing amplitude is evident for cases A and B, in which $h = L_o/2$, and for case C in which $h = L_o/4$. In case D, $h = L_o/10$ and the non-linear wave frequency is greater than the linear value.

Standing Wave Interaction with an Array of Three Submerged Circular Cylinders

In order to demonstrate the flexibility of the mesh generator to model complex geometries, the case of a standing wave in a tank containing three submerged horizontal cylinders was simulated. Figure 5 shows the initial mesh for this case, in which the cylinders each have diameter, $d = 0.35$. The underlying quadtree grid has a maximum of 8 and a minimum of 5 division levels. The wave has an initial cosine elevation of amplitude $a = 0.01$. Figure 6 shows the computed time history of the wave elevation recorded at the centre of the tank. A regular standing wave oscillates above the submerged bodies.

3. CONCLUSIONS

The finite element mesh generator proposed herein produces a mesh of high quality triangular elements without hanging nodes from an underlying quadtree grid. Coupled with the finite element solver, the adaptive grid generator models the moving free surface with a high level of resolution, controlled by the spacing of the seeding points.

The flexibility of the method is demonstrated by the results presented here, which agree well with published data. The predicted deviation of the period of oscillation from the linear value as the wave height is increased corresponds to that described by Tsai and Jeng (1994).

4. ACKNOWLEDGEMENTS

This work forms part of the Uncertainties in Loading on Offshore Structures ULOS programme. It was sponsored by EPSRC through MTD Ltd and jointly funded with: Aker Engineering, Amoco (UK) Exploration Company, BP Exploration Operating Co. Ltd., Brown and Root Ltd., Exxon Production research Company, Health and Safety Executive, Shell UK Exploration and Production, Den Norske Stats Oljeselskap a.s., Texaco Britain Ltd., EPSRC Grant Reference: GR/J23198 (Oxford), GR/J23532 (UCL). The authors would also like to acknowledge the invaluable input provided by Professor R. Eatock Taylor.

5. REFERENCES

Greaves, D.M. (1995) "Numerical modelling of laminar separated flows and inviscid steep waves using adaptive hierarchical meshes", *DPhil thesis*, Oxford University.

Mercer, G.N. and Roberts, A.J. (1992) "Standing waves in deep water: their stability and extreme form", *Physics of Fluids*, Vol. A4(2), pp. 259-269.

Tadjbakhsh, I. and Keller, J. B. (1960) "Standing surface waves of finite amplitude", *Journal of Fluid Mechanics*, Vol. 8, pp. 442-451.

Tsai, C-P. and Jeng, D-S. (1994) "Numerical Fourier solutions of standing waves in finite water depth", *Applied Ocean Research*, Vol. 16, pp. 185-193.

Vanden-Broeck, J-M. and Schwartz, L.W. (1981) "Numerical calculation of standing waves in water of arbitrary uniform depth", *Physics of Fluids*, Vol. 24(5), pp. 812-815.

Wu, G.X. and Eatock Taylor, R. (1995) "Time stepping solutions of the two dimensional non-linear wave radiation problem", *Ocean Engineering*, Vol. 22, pp. 785-798.

Wu, G.X. and Eatock Taylor, R. (1994) "Finite element analysis of two dimensional non-linear Transient water waves", *Applied Ocean Research*, Vol. 16, pp. 363-372.

CASE	h/L_0	H/L_0	(ω/ω_0) present scheme	(ω/ω_0) Tsai and Jeng (1994)
A	0.5	0.05	0.991	0.996
B	0.5	0.13	0.978	0.979
C	0.25	0.10	0.989	0.989
D	0.1	0.02	1.007	1.003

Table 1 Comparison between results predicted by the present method and by Tsai and Jeng (1994) for various combinations of wave steepness and water depth.

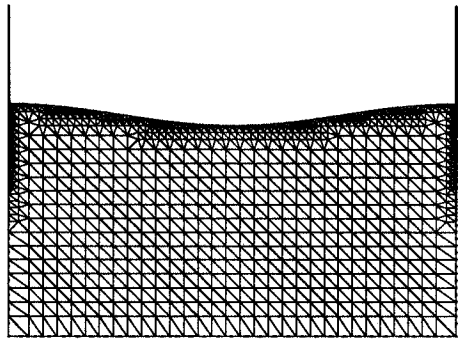

Figure 1 $t = 0$, Case A

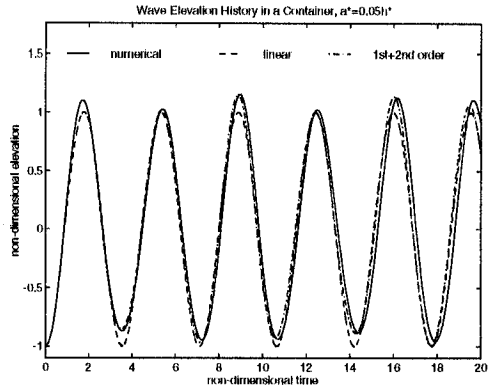

Figure 2 Case A

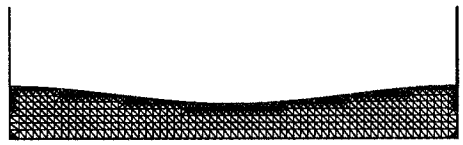

Figure 3 $t = 0$, Case D

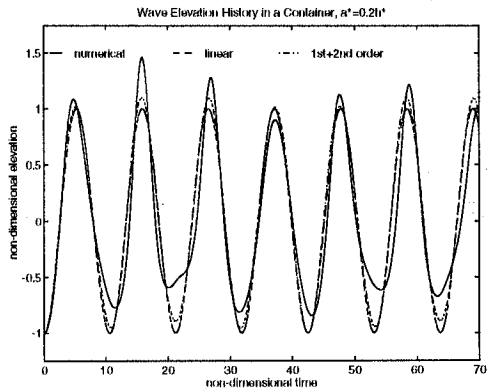

Figure 4 Case D

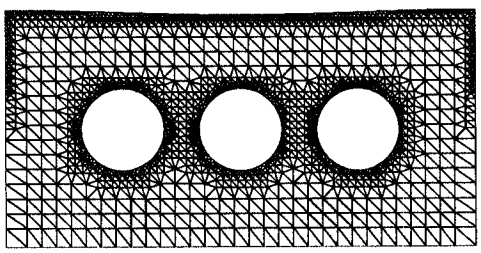

Figure 5 $t = 0$

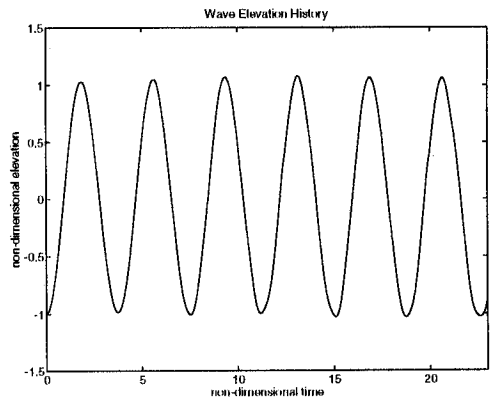

Figure 6 Three submerged circular cylinders

DISCUSSION

Magee A.: Is your gridding scheme appropriate for use in a nonlinear BEM surface grid on a complex (ship) hull form?

Greaves D.M., Borthwick A., Wu G.X.: If a discrete set of seed points can be defined which describe the hull form, then it should be possible to produce a surface mesh using the octree-based method.